NASA TN D-3995

THERMAL CONTROL CONSIDERATIONS FOR A MANNED ORBITING SPACE STATION

By J. Thomas Taylor

Manned Spacecraft Center
Houston, Texas

NATIONAL AERONAUTICS AND SPACE ADMINISTRATION

For sale by the Clearinghouse for Federal Scientific and Technical Information
Springfield, Virginia 22151 – CFSTI price $3.00

ABSTRACT

This report analyzes the advantages of combined passive and active methods for the thermal control of a manned orbital laboratory. The object of the analysis was the reduction of the space radiator heat load by rejecting the heat into space through the module walls. This was done by using external surface coatings. Analyses were conducted on two laboratories, each with crews of 18 and 24 men, at three different power levels. A combination passive and active system is recommended.

CONTENTS

TABLES

FIGURES

THERMAL CONTROL CONSIDERATIONS FOR A MANNED ORBITING SPACE STATION

By J. Thomas Taylor
Manned Spacecraft Center

SUMMARY

This report analyzes the advantages of the combined passive and active methods for thermal control of a manned orbital laboratory. The object of the study was the reduction of the heat load on the space radiators by rejecting some heat through the module walls into space.

The thermal balance on the laboratory included direct solar radiation, reflected solar radiation, and earth infrared radiation in conjunction with internal electrical and metabolic heat loads. The thermal coating effects on the thermal balance and the resulting influences on the heat rejection requirements of two configurations were analyzed for combinations of three electrical power levels, and for a crew of 18 and 24 men.

The proper selection of thermal coatings for exterior surfaces can control structural temperatures. Coating patterns (solar absorptivity and surface emissivity variations about the exterior surface of the space station), resultant heat rejection requirements, and radiator areas and locations are presented.

These considerations favor the selection of combined passive and active methods of controlling temperature and effective heat rejection from the space laboratory. Thermal coating patterns can be applied to achieve the desired passive heat flux from the laboratory modules. Such passive heat losses can substantially reduce the heat rejection requirements imposed on the space radiators, thereby minimizing radiator areas and weights.

INTRODUCTION

The primary purpose of a manned orbiting space station (MOSS) is to conduct laboratory experiments in space for extended periods. Such a station requires a minimum operation of 1 year in a 300-nautical mile earth orbit.

A major requirement is an efficient thermal control system. Long-term operation of the system requires simplicity, reliability, minimum weight, ease of maintenance, and, most importantly, effective and proper control of temperature levels.

Proper temperature control depends upon the effective rejection of heat loads generated from electrical equipment, metabolic processes, and external (sun and earth) heat sources. The lengthy mission virtually precludes any use of expendable fluids for heat rejection. Therefore, ultimate temperature control must be accomplished by rejecting the heat into space.

This paper seeks to show the advantages of the combined passive and active methods of thermal control when applied to a MOSS. The object of the study was the reduction of the heat load on the space radiators by rejecting some heat into space through the module walls. This can be accomplished by selecting proper coatings for the external surface of the MOSS. The passive thermal control design must be compatible with the cabin environmental control design to prevent the inner module wall temperatures from approaching the dewpoint.

A transient analysis was conducted to determine the passive heat flux from the MOSS. The results of this analysis were integrated into a steady-state analysis to determine the approximate radiator sizes and locations. The analyses were conducted for two configurations of the MOSS. A crew of 18 and 24 men, and three levels of electrical power were considered for each configuration.

In this study, no requirements were placed on the system for rejecting the heat that resulted from system inefficiencies. It was assumed that a separate heat rejection system would be provided for this purpose. Thus, thermal control studies relative to the power generation equipment would be included in separate documentation concerning the electrical power system.

SYMBOLS

A albedo of planet

A_P area of plate surface, ft^2

A_R area of radiator surface, ft^2

A_1 surface area of shield, ft^2

A_2 surface area of module wall outer surface, ft^2

C specific heat of subsegment material, Btu/lb-°F

C_p specific heat of radiator fluid, Btu/lb-°F

E_1 planetary infrared radiation, Btu/hr-ft^2

F_A configuration factor for albedo radiation which accounts for solar incident angle over planetary surface

F_{eff} radiative interchange factor

F_i configuration factor for planetary infrared radiation

F_S solar radiation configuration factor

f function of

H_q net heat rejected, Btu/hr-°F

h_c convection heat transfer coefficient, Btu/hr-ft^2-°F

K conductivity of subsegments, Btu/hr-ft^2-°F

ln natural logarithm

Q heat flux, Btu/hr

Q_A planetary albedo radiation absorbed by surface, Btu/hr

Q_i planetary infrared radiation absorbed by surface, Btu/hr

Q_{net} desired heat rejection from the spacecraft, Btu/hr

Q_R heat emitted from surface of plate, Btu/hr

Q_S solar radiation absorbed by surface, Btu/hr

q heat flux per square foot of surface area, Btu/hr-ft^2

S solar constant, 445 Btu/hr-ft^2

T radiator temperature, °R

T_R average temperature of inlet and outlet radiator fluid

$T_{R,1}$ inlet temperature of radiator fluid

$T_{R,2}$ outlet temperature of radiator fluid

T_S effective environmental sink temperature, °R

W weight of subsegment, lb

W_f fluid flow rate, lb/hr

X conductive path length, ft

α surface solar absorptivity

α_i infrared absorptivity of plate surface ($\alpha_i = \epsilon$)

ΔT change in temperature of subdivision during time interval

Δt fluid temperature drop across radiator

ϵ surface emissivity

ϵ_{sw} emissivity of radial configuration shield inner surface and outer surface of cylindrical module

ϵ_1 emissivity of shield outer surface

ϵ_2 emissivity of shield inner surface

ϵ_3 emissivity of module wall outer surface

η_o overall radiator effectiveness

θ time, hr

σ Stefan-Boltzmann constant, 0.173×10^{-8} Btu/hr-ft^2-R^4

τ ratio of radiator temperature to effective environmental sink temperature, T/T_S

τ_1 ratio of $T_{R,1}$ to T_S

τ_2 ratio of $T_{R,2}$ to T_S

ϕ_S angular position in orbit from earth-sun line or subsolar point, deg

ω angle between spin axis and normal to the chord of a segment on module surface, deg

Subscripts:

ave	average
env	environmental temperature in the module
ext	pertains to external conditions
f	final value at end of time interval
i	initial value at beginning of time interval
min	minimum value
1 to 5	pertain to particular subsegments

CONFIGURATIONS AND THERMAL BALANCE MODEL

Hexagonal configurations developed at Langley Research Center (LRC) and radial module (Y) configurations (fig. 1) were chosen for this study. These configurations are representative of the types of space station configurations being considered. The LRC configuration is a hexagon with cylindrical modules making up the sides. These modules are connected to a central hub by three radial components. The Y configuration consists of three radial modules having exterior shields. Typical module cross sections are shown in figure 2.

Each configuration rotates about an axis through the hub, and each axis is parallel to the earth-sun line. The modules are generally of cylindrical shape, or else they can be represented by a cylindrical segment. This shape is the basis for the selection of a thermal balance model. The model was chosen as a cylinder rotating about an axis parallel to the earth-sun line and perpendicular to the longitudinal axis of the cylinder. For the purposes of this paper it was assumed that the orbital plane always contains the earth-sun line. Figure 3 shows the model and pertinent nomenclature.

To establish a thermal balance, the surface of the model was divided into several segments about the circumference (fig. 4). Each segment was considered to be insulated (no conduction) from adjacent segments. Different size segments were chosen for application to the two configurations. Included angles of 30° and 15° were chosen for the segments on the LRC and Y configurations, respectively, as shown in figure 4.

The spin rate of the space station was assumed to be one revolution per degree of orbit. This spin rate was a convenient number for calculations and agreed closely with current thinking on the space station. An average value of the incident external thermal radiation was calculated for each segment at several positions throughout the orbit.

Figure 5 shows typical equilibrium or effective environmental sink temperatures for one half of the orbit. Several such temperature profiles were calculated for various surface emissivities and solar absorptivities. These profiles are useful in the

preliminary selection of thermal coating characteristics, in the calculation of external heat loads, and in the selection of thermal radiator locations.

At this point it may be well to clarify the terms equilibrium temperature and effective environmental sink temperature as used in this report. The equilibrium temperature may be defined as that temperature which a surface would attain if conditions were steady state. In steady-state conditions, the net unbalance in heat exchange between the surface and its environment is zero. The effective environmental sink temperature is equivalent to the equilibrium temperature of a surface insulated on one side and its edges, with this surface receiving radiation only on the other side. The effective environmental sink temperature is analytically defined in appendix A.

ELECTRICAL POWER AND HEAT LOADS

In a parallel space station study, the Manned Spacecraft Center has established three preliminary electrical power levels to meet the requirements of the space station. These power levels, along with the number of men onboard and the type of environmental control system under study, are shown in table I. The power requirements given for the environmental control system were conservatively high, and the portion of the metabolic heat loads to be rejected by the active thermal control system was assumed to be included for purposes of this study. The values given are usable power and must ultimately be converted into heat and rejected by the spacecraft. The heat resulting from the power utilized by the environmental control system was assumed to be rejected essentially by the active thermal control system.

PASSIVE HEAT FLUX ANALYSIS

Since the module cross sections for the two configurations were completely different, a separate approach was followed for each in analyzing the passive heat flux and transient temperatures. An analysis of the two configurations is presented in appendix B.

The LRC configuration was divided into several equivalent flat surfaces (fig. 4). Each surface and its corresponding portion of wall were analyzed separately with various emissivities and solar absorptivities. Surface characteristics were chosen to give the desired passive heat flux out of the module, and to give approximately equal surface temperatures for the various segments.

The Y configuration was analyzed in a somewhat different manner due to the presence of the exterior shield. Irradiation between the inner surface of the shield and the outer surface of the cylindrical module requires a complex analysis to determine the distribution of radiant heat exchange. The actual approach involved arriving at average values of passive heat losses and temperatures about the shield and module walls.

Since each section of outer surface could not be analyzed separately as in the LRC case, it was necessary to approximate the transient temperatures of the shield for proper selection of thermal coatings. Each segment was treated as a thin plate

insulated on the inner surface and insulated from adjacent segments. An analog computer program was set up to calculate the transient temperatures of the segments. These temperatures are a better basis for selection of thermal coatings than are equilibrium temperatures because transient temperatures give a better representation of the actual temperature variation. These data were used to select values of absorptivity and emissivity for calculating average temperatures and passive heat flux over the surface of the shield and module. A more accurate analysis of the configuration would undoubtedly call for some modifications to the surface properties used.

Assumptions

In the analysis of both configurations, it was assumed that the solar constant was equal to 445 Btu/hr-ft^2, that the earth thermal radiation equaled 69 Btu/hr-ft^2, and that the earth-reflected solar radiation equaled 168 Btu/hr-ft^2. The altitude of the circular earth orbit was assumed to be 300 nautical miles with an orbital period of 96 minutes, and a spin rate of one revolution per degree of orbit.

Spacecraft Properties

The module walls have inner and outer aluminum alloy skins 0.05 in. thick, and the outer shield on the Y configuration, only, is 0.05-in. aluminum alloy. (Thermal conductivity equals 90 Btu/hr-ft-°F, density equals 174.5 lb/ft^3, and specific heat equals 0.20 Btu/lb-°F.) The module walls contain 2 in. of polyurethane. (Thermal conductivity equals 0.021 Btu/hr-ft-°F, density equals 1.5 lb/ft^3, and specific heat equals 0.25 Btu/lb-°F.)

Effects of structural members, such as stiffeners, stringers, or honeycomb, on heat transfer are neglected; the internal environment is assumed to be at a constant temperature of 70° F; and the internal heat transfer coefficient h is equal to 0.50 Btu/hr-ft^2-°F. This value is considered conservative due to the required convective flow in the space station.

Allowable Passive Heat Loss

As indicated in the introduction, the heat load on the space radiators was to be reduced by rejecting some heat into space through the module walls. In the final design of the MOSS it will be necessary to determine allowable heat loss from each module.

In this study, the relatively constant electrical load (other than the environmental control system) in a module presented itself as a basis for allowable heat loss. Table II presents a breakdown per module of the three power levels used. It was assumed that all heat loads except those realized from the crew and environmental control system were dispersed equally throughout the modules.

Radial (Y) Configuration

Table II(a) shows that the electrical power loads, other than for environmental control, result in 12 514, 10 239, and 17 065 Btu/hr for power levels 1, 2, and 3, respectively. Dissipating all of this heat passively based on a 2600-square-foot module area results in average heat fluxes of 4.81, 3.94, and 6.53 Btu/hr-ft^2 for power levels 1, 2, and 3, respectively. Three sets of passive heat loss curves are shown in figure 6. The heat loss was determined for three exterior surface coating patterns using two values of emissivity ϵ_{sw} of the inner shield surface and outer surface of the cylindrical module. The three coating patterns and average heat losses over the surface are given in tables III and IV. From table IV, pattern 3 ($\epsilon_{sw} = 0.90$) results in an average heat loss of 4.60 Btu/hr-ft^2, which reasonably satisfies power level 1; pattern 3 ($\epsilon_{sw} = 0.30$) results in an average heat loss of 3.52 Btu/hr-ft^2, which reasonably satisfies power level 2; and pattern 2 ($\epsilon_{sw} = 0.90$) results in an average flux of 5.99 Btu/hr-ft^2, which reasonably satisfies the allowable heat loss established for power level 3. Figure 7 shows the effective environmental sink temperatures or steady-state equilibrium temperatures for the coating patterns chosen (table V). The average external heat absorbed by the shield for the three patterns is shown in figure 8. Figures 9, 10, and 11 present the transient periodic temperatures of the shield and module wall for the coating patterns considered.

Langley Research Center (LRC) Configuration

The electrical loads assumed to be the allowable heat loss are given in table II(b) as 2.60, 2.13, and 3.56 Btu/hr-ft^2 for power levels 1, 2, and 3, respectively. As a result of the similarity in the allowable heat losses of power levels 1 and 2, a single coating pattern was arrived at for both power levels (table VI). Figure 12 shows the transient surface temperatures for the two power levels, and figure 13 presents the passive heat flux out from the module for each of the surface segments throughout an orbit. The average passive heat flux per orbit for each surface segment is given in table VI, and figure 14 shows the average periodic heat loss and average temperature over the surface of the module. The overall average heat loss is 2.57 Btu/hr-ft^2 (table VII). This results in a total heat loss of 6168 Btu/hr, as compared with 6246 Btu/hr and 5120 Btu/hr for the allowable heat losses for power levels 1 and 2, respectively.

Figure 15 shows the transient surface temperatures for power level 3, and table VI shows the coating pattern. The passive heat losses for the surfaces are shown in figure 16, and the average passive heat loss for each surface is shown in table VI. Figure 17 shows the average periodic heat loss and average temperature over the surface of the module. The overall average heat loss is 3.67 Btu/hr-ft^2 (table VII) or a total of 8808 Btu/hr. This compares reasonably well with the allowable heat loss of 8532 Btu/hr as given in table II(b). Figure 18 presents transient temperatures of two wall segments, 180° apart.

RADIATOR ANALYSIS

The objective of this analysis was to specify locations and minimum radiator areas to meet the space station heat rejection requirement (appendix C). The results of the passive heat flux analysis have been integrated into this analysis to reduce the heat rejection requirements on the radiators. However, radiator areas necessary to reject the total internal heat load in a module are presented for purposes of comparison. No effort was made to optimize the radiators or to make a transient analysis.

Assumptions

The radiator fin efficiency is assumed to be 100 percent, with the design point coinciding with the maximum effective environmental sink temperature. The solar absorptivity α is assumed to be 0.18, and the surface emissivity ϵ is assumed to be 0.90. The film coefficient between the radiator fluid and tube surface is assumed to be infinite; that is, there is no temperature drop between the fluid and the radiator. It is further assumed that all surfaces radiate diffusely, that the irradiation from vehicle surfaces to the radiator is negligible, and that the environmental control and the electrical equipment coolant loops comprise one system and use one common radiator panel.

Radiator Location

The selection of a location for a thermal radiator is dependent, to a large extent, on the effective environmental sink temperature. On the basis of low maximum environmental sink temperatures, the locations of flat radiator areas having angles of 90° and 150° between normals to their surfaces and the spin axis are the most promising.

Exterior appendages will restrict location of the radiators. However, such appendages have not been considered in this study. The exterior shape of the Y configuration makes it necessary to deploy radiators for the locations considered, except for the flat shield surfaces which have an angle of 150° between the normal and the earth-sun line. There is also a small amount of available area on the outer end of the module. This area is in a plane parallel to the spin axis. Since the sink temperature varies only slightly, the area-to-heat flux ratios are given for the average orbital environmental sink temperature.

Ratio of Radiator Area to Heat Rejection

Figure 19 presents the ratio of radiator area to heat flux for various inlet and outlet radiator fluid temperatures. These ratios are given for the points of maximum environmental sink temperature, with the exception of the location angle of 90°.

Radiators for Maximum Heat Rejection

For purposes of comparison, radiator areas for maximum heat rejection were found. The maximum heat rejection was assumed to be the total internal heat load without any net heat gain or heat loss in the module. The maximum heat loads are given as total Btu/hr in table II.

Figure 20(a) shows the radiator areas necessary to reject the maximum heat loads in a Y configuration module for the three power levels. The areas are given for inlet radiator fluid temperatures of 60°, 80°, and 100° F and a constant outlet temperature of 40° F. Of the surface locations considered, those having location angles of 90° result in the smallest radiator areas. The smallest area of 255 square feet occurs at power level 1 and an inlet temperature of 100° F. The maximum rectangular area available on the outer end of the module is approximately 157 square feet. The 150° surfaces are the only locations which can accommodate the radiator areas without deploying them. However, approximately a 1117-square-foot area is available on each of the 150° surfaces.

Figure 20(b) shows that the same general trend of radiator areas holds for the LRC configuration. For the locations considered, the smallest area available is for power level 1.

Heat Rejection With Passive Heat Flux

Selection of coating patterns and the resulting passive heat flux was discussed in a previous section. Tables V and VII give the net heat remaining in a module after the maximum allowable passive heat losses have been considered. This heat must be dissipated by the thermal control system.

The Y configuration radiator areas are shown in figure 21(a) for the three power levels and location angles considered. Of the locations considered, the smallest areas are obtained at a location angle of 90°. All of the areas for power level 1 (fig. 21(a)) at a location angle of 90° can be located on the outer end of the module. Ample area is available on the 150° surfaces of the shield for all power levels.

Radiator area requirements for the LRC configuration are shown in figure 21(b) for the locations considered. The smallest area of 130 square feet with an inlet temperature of 100° F occurs for power level 1. Each location was based on a 30° included angle, and an area of approximately 194 square feet is available at each. The chord length of each of these segments is approximately 2.59 feet. However, since this dimension would lead to an impractical radiator design, final design and location will probably encompass area from more than one of the segments assumed for this analysis.

FINAL DESIGN CONSIDERATIONS

Thermal control coatings for passive control of heat flux must be selected not only for heat balance design but also to minimize degradation of coating materials and to reduce temperature gradients for increased structural integrity.

The heat transfer coefficient between the inner module wall and the module atmosphere will influence the exterior surface coating design. The passive thermal control design must be compatible with the design of the environmental control system to insure that inner wall temperatures will not reach the dewpoint which would cause condensation on the walls. The dewpoint of the space station will probably be in the range of 50° to 55° F. The wall temperatures found for the LRC configuration are above this temperature, but the Y configuration wall temperatures found in the analysis are very close to this 50° to 55° F temperature range. Condensation could become a problem if the internal heat transfer coefficient is not increased above the value of 0.50 Btu/hr-ft^2-°F used in this analysis.

Final radiator design will be greatly influenced by transport fluid, allowable pressure drops and flow rates necessary to maintain internal temperatures, overall design of the environmental control system, coolant loops for equipment which cannot be cooled passively, and possible integration of the power system thermal control with that of the electrical equipment and environmental control system.

Studies must be carried out to establish requirements for meteoroid protection and methods of leak detection for the radiators. It will also be necessary to determine whether the transport fluid might freeze in the radiators; if so, methods for eliminating this problem should be found.

CONCLUDING REMARKS

A combination of passive and active methods is recommended for thermal control of the space station. Thermal coating patterns can be applied to achieve the desired passive heat flux from the station modules. Such passive heat losses can substantially reduce the heat rejection requirements imposed on the space radiators, thereby minimizing radiator areas and weights.

Neglecting the possibility of external appendages and radiator deployment, radiator area requirements tend to be minimized by locating the radiators with an angle of 90° between the spin axis and the normal to the radiator surface. The preceding conclusion is based on a steady-state analysis. The final design of the space radiators must be based on a transient operational analysis. A radiator located at 150° experiences lower sink temperatures throughout a greater portion of the orbit than does a radiator located at 90°. A transient analysis will probably show that a smaller area than that found in the steady-state analysis can be used at 150°, since the surface experiences the maximum sink temperature for only a short period. Thus, the results of this phase of the study are conservative.

The Y configuration offers sufficient area for radiator locations on the 150° shield surfaces. The 157-square-foot area on the outer ends of the modules can be utilized for radiators having inlet temperatures of 100°, 80°, and 60° F with outlet temperatures of 40° F, and heat rejection requirements of approximately 13 826 Btu/hr each.

Sufficient radiator area is available on the outer surface of the LRC modules. Radiator areas given in this report are based on flat surface areas for given locations.

Manned Spacecraft Center
National Aeronautics and Space Administration
Houston, Texas, January 26, 1967
981-10-10-05-72

APPENDIX A

THERMAL EQUILIBRIUM (STEADY-STATE) ANALYSIS OF A THIN FLAT PLATE IN THE SPACE ENVIRONMENT, COMPLETELY INSULATED ON ONE SIDE AND ALL EDGES

The following analysis predicts the effective environmental sink temperature and the associated heat flux from the space environment. The external heat flux includes solar radiation, planetary infrared radiation, and planetary albedo radiation.

Heat Balance on Flat Plate

In the equation

$$Q_R = Q_S + Q_A + Q_i \tag{A1a}$$

heat emitted equals heat absorbed, where

$Q_R = \epsilon\sigma A_P T_S^4$, Btu/hr, heat emitted from surface of plate

$Q_S = \alpha F_S S A_P$, Btu/hr, solar radiation absorbed by surface

$Q_A = \alpha F_A A S A_P$, Btu/hr, planetary albedo radiation absorbed by surface

$Q_i = \alpha_i F_i E_i A_P$, Btu/hr, planetary infrared radiation absorbed by surface

The effective environmental sink or equilibrium temperature is derived as follows:

$$\epsilon\sigma A_P T_S^4 = \alpha F_S S A_P + \alpha F_A A S A_P + \alpha_i F_i E_i A_P \tag{A1b}$$

or

$$T_S = \left\{ \frac{1}{\sigma} \left[\frac{\alpha}{\epsilon} \left(F_S S + F_A A S \right) + F_i E_i \right] \right\}^{1/4} \tag{A2}$$

where

$$\alpha_i \simeq \epsilon$$

The external heat flux can be found from

$$Q_{ext} = Q_S + Q_A + Q_i \tag{A3}$$

or by

$$Q_{ext} = \epsilon \sigma A_P T_S^{\ 4} \tag{A4}$$

The preceding analysis is convenient for analyzing the combined effects of solar radiation, planetary infrared radiation, and planetary albedo radiation absorbed by a surface. Use of the absorbed radiation in the form of an effective environmental sink temperature also facilitates analysis of the transient response of the structure under study to changes in its environment. By establishing an orbital profile of effective environmental sink temperatures (no net heat transferred) for a given surface, equation (A4) can be utilized to provide the time variation of external heat absorbed by the surface.

The usefulness of the environmental sink temperature in space radiator analyses is discussed in appendix C.

APPENDIX B

PASSIVE HEAT FLUX ANALYSES OF SPACE STATION MODULES

The analyses presented are directed toward approximating wall temperatures and the passive heat flux of manned space stations in the space environment. The analyses are useful in selecting spacecraft thermal coatings for desired temperature levels and predicting the heat balance between external heat received and internal heat loads.

Cylindrical Module (Applicable to the LRC Configuration)

The following is a one-dimensional transient analysis for approximating the heat flux and wall temperatures of a cylindrical module with a known internal environment (assumed constant). The analysis is further simplified by dividing the circumference of the wall into several flat plate segments and treating each segment independently; that is, each segment is completely insulated from adjacent segments. This also allows selection of appropriate thermal coating characteristics for each segment to control wall temperatures and heat flux. It is assumed in the analysis that the time interval $\Delta\theta$ is sufficiently small such that the temperature differences at the beginning of the time interval and the temperature differences at the end of the time interval are not sufficiently different to produce a significant error.

To determine the heat balance on the wall segment (see sketch below showing module wall cross sections and temperature locations), assume that the wall segment

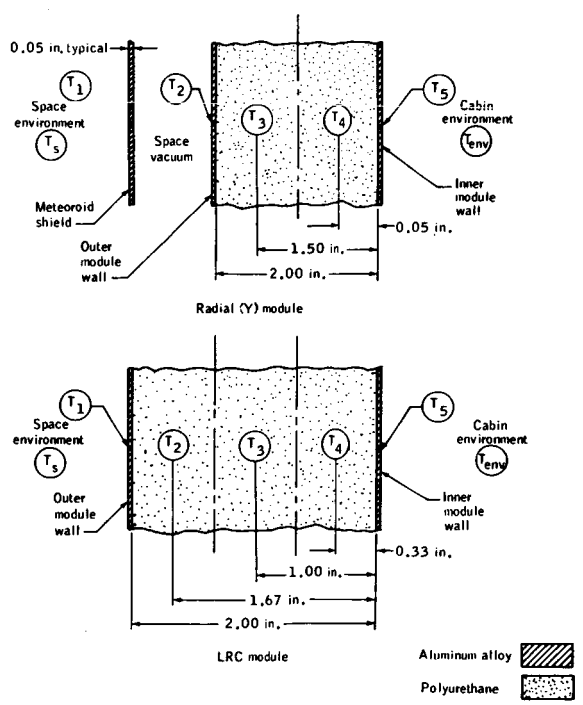

heat transfer area is 1 square foot, and subdivide the wall into several parallel subsegments through the wall thickness. Thus the heat balance for a small time interval $\Delta\theta$ on the outer aluminum alloy skin (thermally thin, that is, no ΔT across skin) becomes

(heat stored by skin) = (external heat absorbed)

+ (heat to or from the adjacent subsegment by conduction)

- (heat emitted from the outer surface of the skin)

or by

$$W_1 C_1 \frac{\Delta T_1}{\Delta\theta} = \left(Q_{ext}\right)_{ave} + \frac{K}{X_{21}}\left(T_{2i} - T_{1i}\right) - \epsilon\sigma T_{1i}^{4} \tag{B1}$$

The heat balance on the inner module aluminum alloy skin is

(heat stored by skin) = (heat transferred from the module internal environment by convection)

+ (heat transferred to or from adjacent subsegment by conduction)

or

$$W_5 C_5 \frac{\Delta T_5}{\Delta\theta} = h_c\left(T_{env} - T_{5i}\right) - \frac{K}{X_{54}}\left(T_{5i} - T_{4i}\right) \tag{B2}$$

The heat balance on all internal subdivisions of the wall, denoted by subscripts 2, 3, and 4, is influenced only by conduction, and can be written in the general form

$$W_y C_y \frac{\Delta T_u}{\Delta\theta} = \frac{K}{X_{zy}}\left(T_{zi} - T_{yi}\right) - \frac{K}{X_{xy}}\left(T_{yi} - T_{xi}\right) \tag{B3}$$

where the subscripts x, y, and z indicate adjacent subdivisions. The analysis as used in this study includes three equations of the above form.

The heat loss by the internal module environment at any instant is

$$q = h_c \left(T_{env} - T_5\right) \frac{\text{Btu}}{\text{hr-ft}^2} \tag{B4}$$

The above analysis requires that the weight, specific heat, conductivity, conductive path length, and initial temperature of each subsegment be defined. Also, it is assumed that the internal temperature T_{env} and outer skin emissivity and solar absorptivity are known. The external heat flux can be found as discussed in appendix A and averaged over the time interval $\Delta\theta$ being considered. An iterative type analysis must then be carried out over the orbital time period until the temperature profile of each subsegment becomes periodically stable.

The remaining or net heat load in the module is found by summing the average passive heat flux for the orbital period of each segment of the module, and comparing with the known internal heat loads (electrical and metabolic):

$$Q_{net} = \text{(electrical heat load)} + \text{(metabolic heat load)} - \text{(passive heat flux)}$$

This net heat load must be rejected by an active thermal control system. Thermal space radiators for rejection of this net heat load are discussed in appendix C.

Cylindrical Module With Thin Aluminum Alloy Shield (Applicable to the Radial Configuration)

Analysis of a cylindrical module with an exterior shield becomes complex if the surface of the module is analyzed in segments, as in the case of a cylinder. This is due primarily to the complex irradiation between the inner surface of the shield and outer surface of the cylindrical module. The thermal analysis can be simplified by selecting thermal coating characteristics for the outer surface of the shield to approach an isothermal condition about the shield at any given time. An approximation of the passive heat flux to and from the module can be obtained by treating the radiant interchange between the module and shield as an enclosed body radiating to its enclosure and by analyzing the complete module. The subdivision of the module wall and shield for purposes of analysis is shown in the previous sketch. The same assumptions regarding $\Delta\theta$ and ΔT as stated previously apply in this analysis.

The net exchange of heat between the module and shield can be expressed by Christiansen's equation (ref. 1):

$$Q_{21} = \frac{\epsilon_1^{\,2}}{1 + \epsilon_3\left(\frac{1}{\epsilon_2} - 1\right)\frac{A_2}{A_1}} \sigma A_2 \left(T_2^{\,4} - T_1^{\,4}\right) \tag{B5a}$$

or

$$Q_{21} = F_{eff}\epsilon_3\sigma A_2\left(T_2^4 - T_1^4\right) \tag{B5b}$$

where

$$F_{eff} = \frac{1}{1 + \epsilon_3\left(\frac{1}{\epsilon_2} - 1\right)\frac{A_2}{A_1}}$$

The heat balance on the shield (thermally thin) can now be written for the time interval $\Delta\theta$:

(net heat stored in shield) = (external heat absorbed by shield)

+ (heat transferred by radiation from module)

- (heat emitted from shield outer surface to the space environment)

$$W_1C_1A_1\frac{\Delta T_1}{\Delta\theta} = A_1Q_{ext} + F_{eff}\epsilon_3\sigma A_2\left(T_{2i}^4 - T_{1i}^4\right) - \epsilon_1\sigma A_1T_{1i}^4 \tag{B6a}$$

or

$$W_1C_1\frac{\Delta T_1}{\Delta\theta} = Q_{ext} + \frac{A_2}{A_1}F_{eff}\epsilon_3\sigma T_{2i}^4 - \sigma T_{1i}^4\left(\frac{A_2}{A_1}F_{eff}\epsilon_3 + \epsilon_1\right) \tag{B6b}$$

where Q_{ext} is the average external heat flux over the entire shield surface for the time interval $\Delta\theta$.

The heat balance on the module outer aluminum skin (assumed thermally thin) can be written

$$W_2 C_2 \frac{\Delta T_2}{\Delta \theta} = \frac{K}{X_{32}} \left(T_{3i} - T_{2i} \right) - F_{eff} \epsilon_3 \sigma \left(T_{2i}^{\ 4} - T_{1i}^{\ 4} \right) \qquad \text{(B7)}$$

where the first term on the right side of equation (B7) is the conductive heat exchange between the module outer aluminum skin and its adjacent (polyurethane) subsegment. The second term on the right side of equation (B7) represents the radiant interchange between the shield inner surface and module outer surface.

The heat balance on the inner wall subsegments and module inner skin are the same form as equations (B3) and (B2), respectively. The heat flux to and from the inside of the module can be expressed by equation (B4). An iterative analysis as previously described for the LRC configuration must be performed.

The remaining heat in the module which must be rejected by the active system is

$$Q_{net} = \text{(electrical heat load)} + \text{(metabolic heat load)} - \text{(passive heat flux)} \qquad \text{(B8)}$$

The passive heat flux as given by equation (B4) must be averaged over the orbital time period for the entire module surface.

APPENDIX C

RADIATOR THERMAL ANALYSIS

The following analysis predicts the minimum radiator area necessary to reject a known quantity of heat for given radiator fluid temperatures and space environment conditions.

The thermal balance of the radiator surface can be written

$$Q_{net} = Q_R - \left(Q_S + Q_A + Q_i\right) \tag{C1}$$

where

Q_{net} = the desired heat rejection from the spacecraft, Btu/hr

Equation (C1) may also be written

$$Q_{net} = \epsilon\sigma A_R T^4 - Q_{ext} \tag{C2a}$$

where Q_{ext} is as defined in appendix A. Therefore

$$Q_{net} = \epsilon\sigma A_R T^4 - \epsilon\sigma A_R T_S^{\ 4} = \epsilon\sigma A_R \left(T^4 - T_S^{\ 4}\right) \tag{C2b}$$

The net heat rejection in terms of the radiator heat transport fluids is

$$Q_{net} = W_f C_p \left(T_{R,1} - T_{R,2}\right) \tag{C3}$$

where

W_f = fluid flow rate, lb/hr

C_p = specific heat of, Btu/lb-°F

$T_{R,1}$ = inlet temperature of fluid to radiator, °R

$T_{R,2}$ = outlet temperature of fluid from radiator, °R

In order to apply equation (C2b) to a fin-tube type radiator the equation must be written

$$Q_{net} = \epsilon\sigma A_R \eta_o \left(T^4 - T_S^4\right) \tag{C4}$$

The term η_o is defined as the overall radiator effectiveness and accounts for temperature distributions and heat transfer in the extended surfaces (fins). An isothermal radiating surface would have an overall effectiveness of 1.0. A more complete definition is presented in reference 2.

Considering an element of radiator surface, equation (C3) becomes

$$dQ_{net} = -W_f C_p dT_R \tag{C5}$$

and equation (C4) becomes

$$dQ_{net} = \epsilon\sigma\eta_o \left(T^4 - T_S^4\right) dA_R \tag{C6a}$$

Assuming there is no temperature drop from the bulk fluid to the outer tube-wall surface, $T = T_R$ and $dT = dT_R$. Combining equations (C5) and (C6a) results in

$$W_f C_p \, dT = \epsilon \sigma \eta_o \left(T^4 - T_S^4 \right) dA_R \tag{C6b}$$

or

$$\int_{T_{R,2}}^{T_{R,1}} \frac{dT}{\left(T^4 - T_S^4 \right)} = \frac{\epsilon \sigma \eta_o}{W_f C_p} \int dA_R \tag{C6c}$$

Substituting τ for $\frac{T}{T_S}$, τ_1 for $\frac{T_{R,1}}{T_S}$, τ_2 for $\frac{T_{R,2}}{T_S}$, and integrating, the following equation is obtained:

$$\frac{\epsilon \sigma \eta_o T_S^3 A_R}{W_f C_p} = f(\tau_2) - f(\tau_1) \tag{C7a}$$

where

$$f(\tau) = \frac{1}{4} \ln \left| \frac{\tau + 1}{\tau - 1} \right| + \frac{1}{2} \tan^{-1} \tau$$

The analysis up to equation (C7a) is explained more fully in reference 2.

To simplify the analysis and neglect the use of a specific transport fluid, remembering $T = T_R$, equation (C7a) can be written

$$\frac{\epsilon \sigma \eta_o T_S^3 A_R}{W_f C_p \Delta t} = \frac{f(\tau_2) - f(\tau_1)}{\Delta t} \tag{C7b}$$

where Δt is the temperature drop from inlet to outlet of the radiator transport fluid. Therefore, the denominator on the left side of equation (C7b) becomes $W_f C_p \Delta t$, which is equal to Q_{net}, and $\Delta t = T_{R,1} - T_{R,2}$. Equation (C7b) becomes

$$\frac{\epsilon \sigma \eta_o T_S^3 A_R}{Q_{net}} = \frac{f(\tau_2) - f(\tau_1)}{\Delta t} \tag{C8}$$

Assuming Q_{net}, $T_{R,1}$, $T_{R,2}$, T_S, and ϵ, equation (C8) yields the radiator area for the required heat rejection Q_{net} to the space environment. The minimum radiator area to accomplish a given heat rejection is obtained if the overall radiator effectiveness η_o is 1.0.

$$(A_R)_{min} = \left[f(\tau_2) - f(\tau_1)\right] \frac{Q_{net}}{\epsilon \sigma T_S^3 \Delta t} \tag{C9}$$

REFERENCES

1. Jakob, Max: Heat Transfer. Vol. II, John Wiley and Sons, Inc., Dec. 1959.

2. The Garrett Corp., AiResearch Manufacturing Division. Radiator Design for Space Vehicle. (Rev. 1) Rep No. STC-20-R; July 1962.

TABLE I. - ESTIMATED POWER LEVELS

Power level	Usable power, kW	Type ECS	Number of men	ECS power, kW	ECS power/man		Other electrical power, kW
					kW	Btu/hr	
1	18	Rechargeable	18	7	0.3888	1327.2	11
2	27	Regenerative	18	18	1.0000	3413.0	9
3	40	Regenerative	24	25	1.0416	3555.0	15

TABLE II. - MAXIMUM INTERNAL HEAT LOADS PER MODULE

(a) Y configuration (area - 2600 ft^2)

Power level	Number of men	ECS power		Other electrical power			Total Btu/hr
		kW	Btu/hr	kW	Btu/hr	Btu/hr-ft^2	
1	10	3.88	13 272	3.66	12 514	4.81	25 786
2	10	10.00	34 130	3.00	10 239	3.94	44 369
3	10	10.416	35 550	5.00	17 065	6.53	52 615

(b) LRC configuration (area - 2400 ft^2)

Power level	Number of men	ECS power		Other electrical power			Total Btu/hr
		kW	Btu/hr	kW	Btu/hr	Btu/hr-ft^2	
1	10	3.88	13 272	1.83	6246	2.60	19 518
2	10	10.00	34 130	1.50	5120	2.13	39 250
3	10	10.416	35 550	2.50	8532	3.56	44 082

TABLE III. - RADIAL CONFIGURATION COATING PATTERNS

Location, ω, deg	Pattern 1		Pattern 2		Pattern 3	
	$\frac{\alpha}{\epsilon}$	ϵ	$\frac{\alpha}{\epsilon}$	ϵ	$\frac{\alpha}{\epsilon}$	ϵ
7.5	0.17	0.90	0.22	0.90	0.27	0.90
22.5	.19	.90	.24	.90	.29	.90
37.5	.20	.90	.26	.90	.32	.90
52.5	.24	.90	.32	.90	.41	.90
150.0	.87	.85	1.09	.80	1.38	.60

TABLE IV. - RADIAL CONFIGURATION PASSIVE HEAT LOSS PER MODULE

Pattern	Average heat loss, Btu/hr-ft^2		Average heat loss, Btu/hr	
	$\epsilon_{sw} = 0.30$	$\epsilon_{sw} = 0.90$	$\epsilon_{sw} = 0.30$	$\epsilon_{sw} = 0.90$
1	5.33	7.15	13 861	18 590
2	4.53	5.99	11 778	15 574
3	3.52	4.60	9 152	11 960

TABLE V. - RADIAL CONFIGURATION ACTIVE HEAT LOADS PER MODULE FOR SELECTED COATING PATTERNS

Power level	Pattern	ϵ_{sw}	Average passive heat loss, Btu/hr-ft^2	Average passive heat loss, Btu/hr	Active heat load, Btu/hr
1	3	0.90	4.60	11 960	13 826
2	3	.30	3.52	9 152	35 217
3	2	.90	5.99	15 574	37 041

TABLE VI. - LRC CONFIGURATION COATING PATTERNS

AND AVERAGE PASSIVE HEAT LOSS PER SEGMENT

Location, ω, deg	Power levels 1 and 2			Power level 3		
	$\frac{\alpha}{\epsilon}$	ϵ	Heat loss, Btu/hr-ft^2	$\frac{\alpha}{\epsilon}$	ϵ	Heat loss, Btu/hr-ft^2
0	0.30	0.30	2.52	0.30	0.90	3.13
30	.30	.30	3.44	.35	.90	3.27
60	.50	.30	3.56	.55	.50	3.45
90	2.50	.10	1.67	2.00	.40	4.50
120	3.00	.10	2.37	2.50	.20	3.89
150	2.50	.10	1.65	2.00	.20	3.52
180	1.50	.10	2.92	1.50	.15	3.59

TABLE VII. - LRC CONFIGURATION AVERAGE PASSIVE HEAT LOSS

AND ACTIVE HEAT LOADS PER MODULE

Power level	Average passive heat loss, Btu/hr-ft^2	Average passive heat loss, Btu/hr	Active heat load, Btu/hr
1	2.57	6168	13 350
2	2.57	6168	33 082
3	3.67	8808	35 274

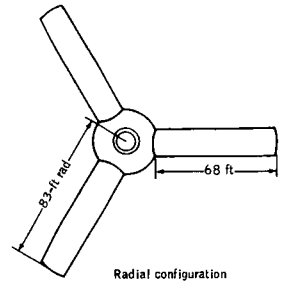

Radial configuration

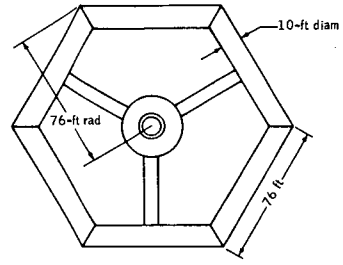

LRC configuration

Figure 1. - Radial and LRC configurations.

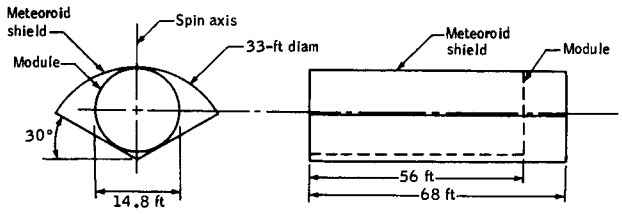

Radial (Y) module

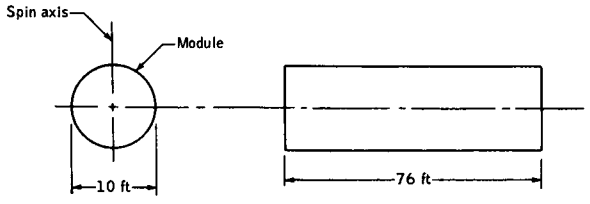

LRC module

Figure 2. - Typical module cross sections.

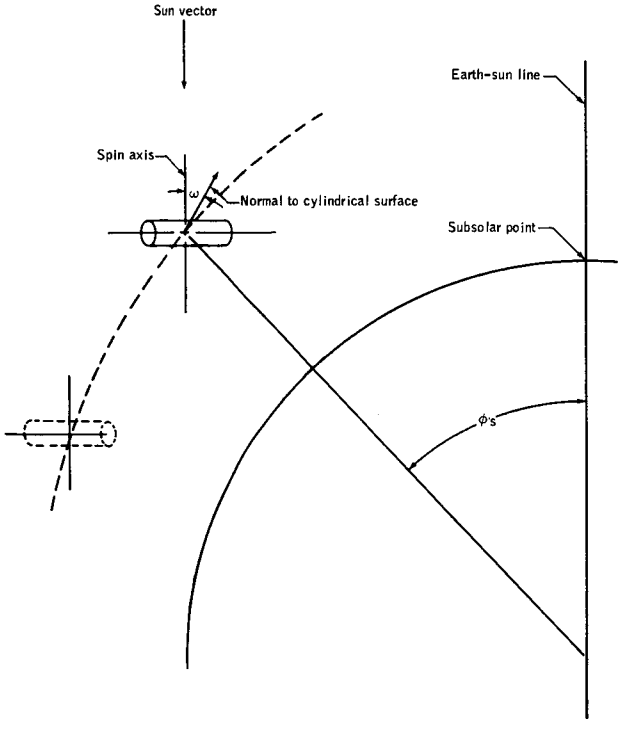

Figure 3. - Basic thermal model.

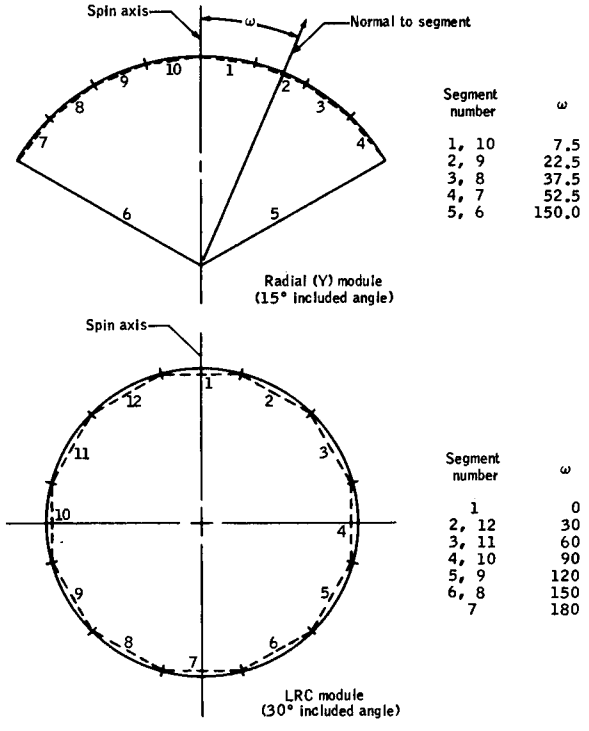

Segment number	ω
1, 10	7.5
2, 9	22.5
3, 8	37.5
4, 7	52.5
5, 6	150.0

Segment number	ω
1	0
2, 12	30
3, 11	60
4, 10	90
5, 9	120
6, 8	150
7	180

Figure 4. - Radial and LRC module segment locations.

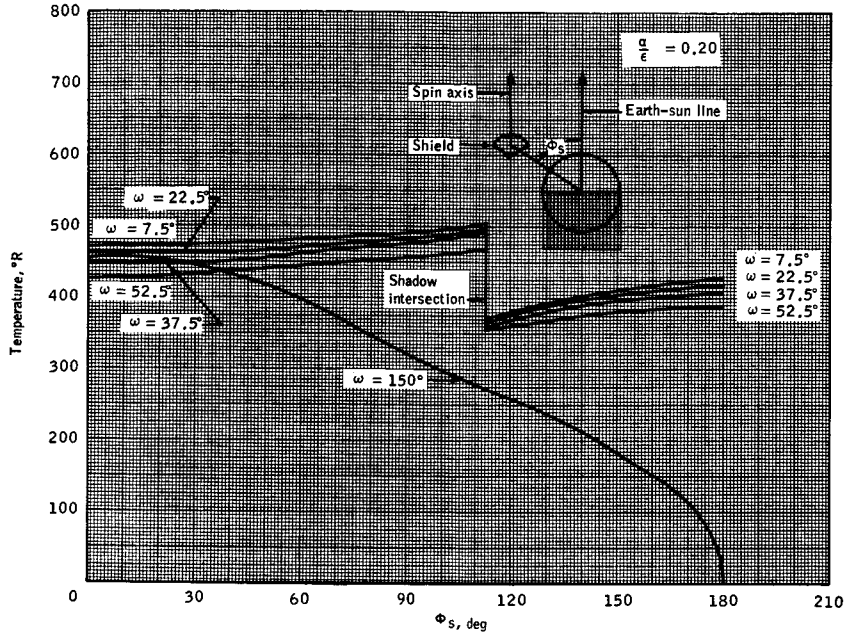

(a) Radial module temperatures.

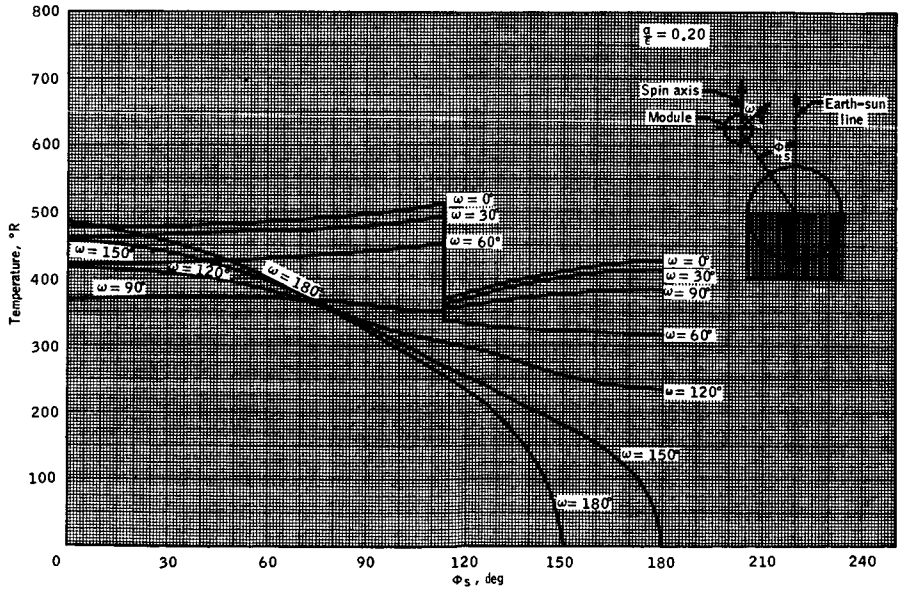

(b) LRC module temperatures.

Figure 5. - Typical equilibrium temperatures.

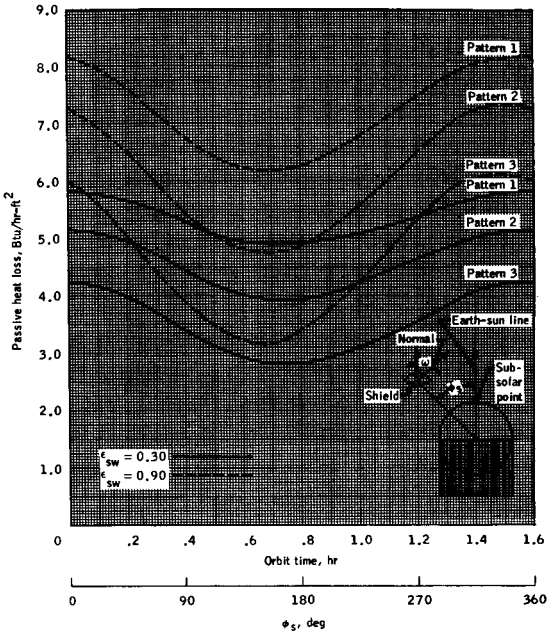

Figure 6. - Radial configuration passive heat loss from module. (See table III for pattern data.)

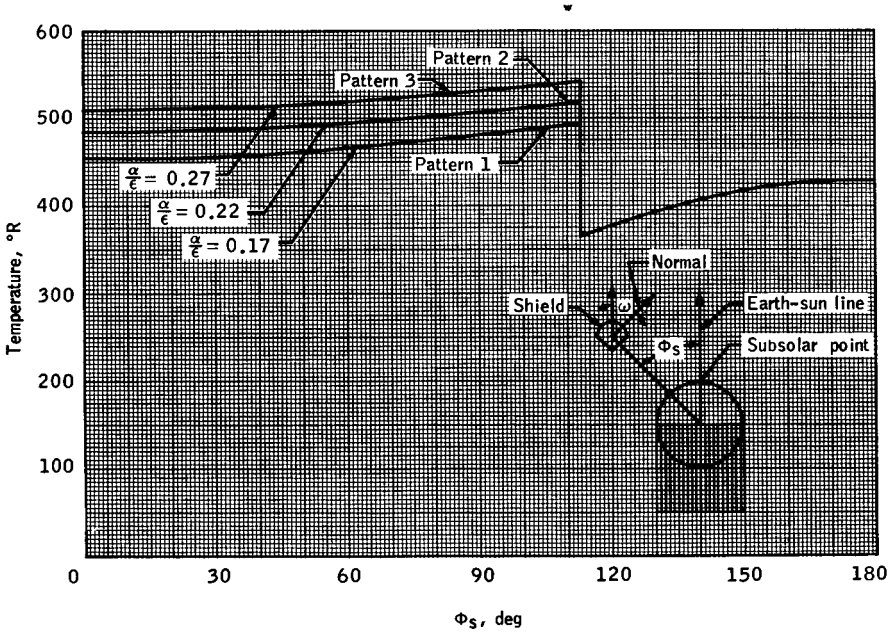

(a) $\omega = 7.5°$.

Figure 7. - Radial configuration equilibrium temperatures for patterns 1, 2, and 3. (See table III for pattern data.)

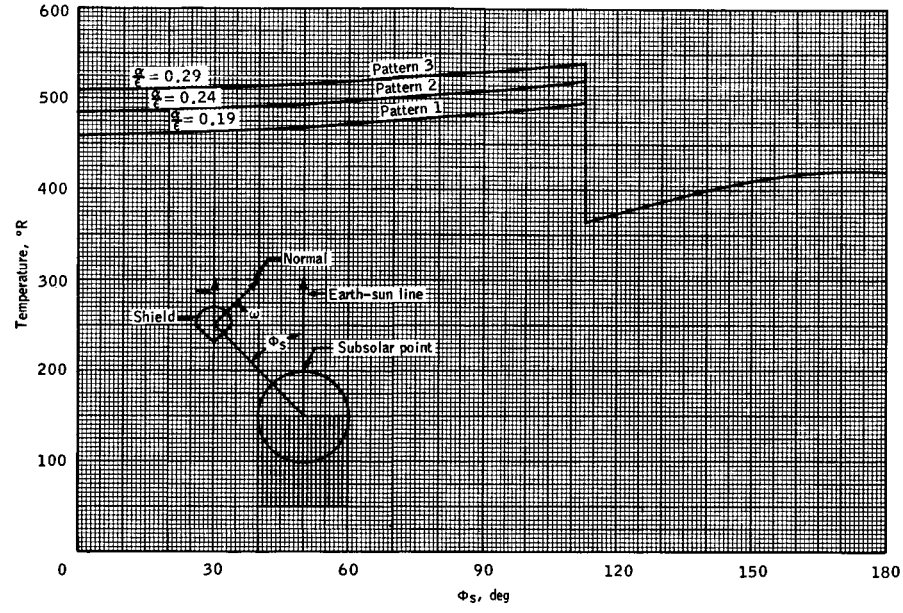

(b) $\omega = 22.5°$.

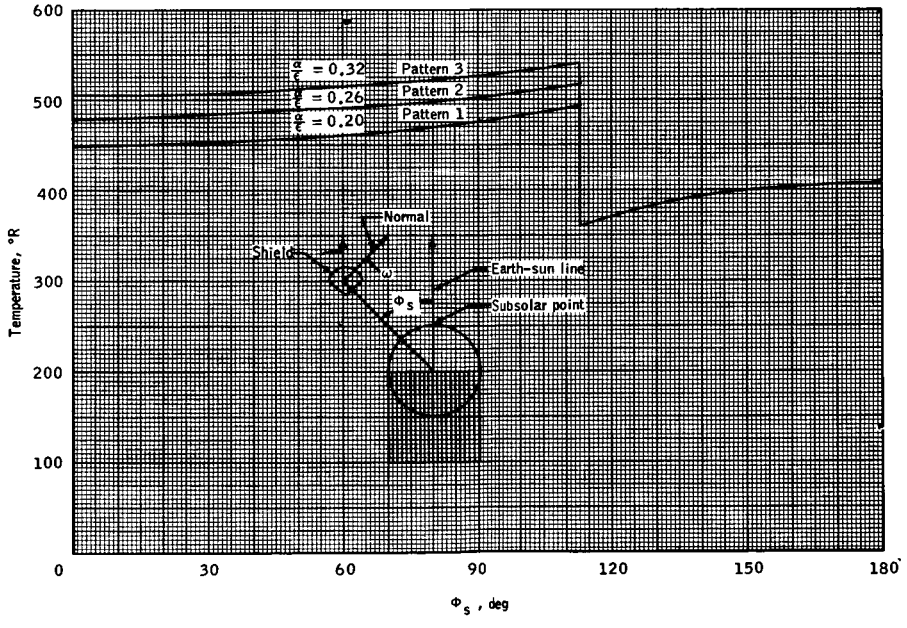

(c) $\omega = 37.5°$.

Figure 7. - Continued.

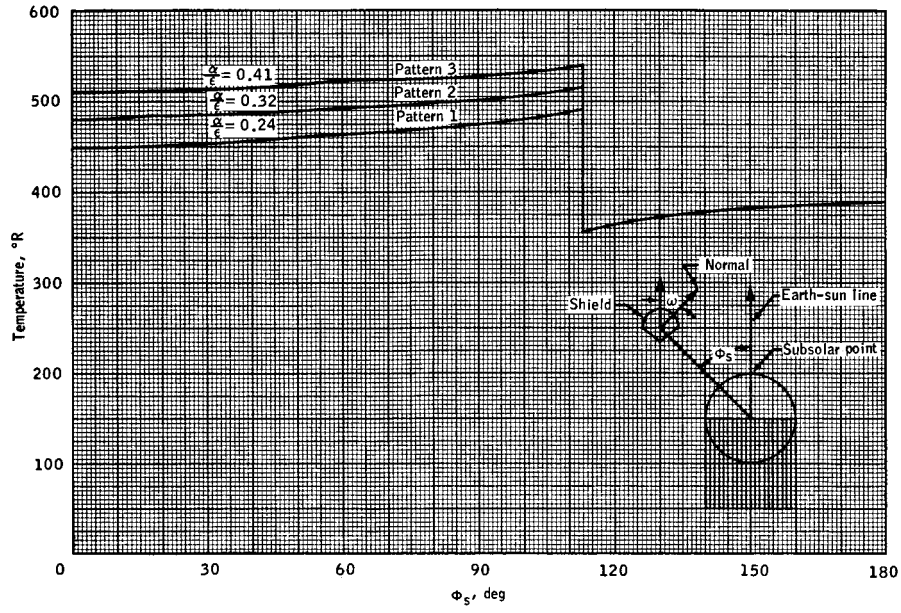

(d) $\omega = 52.5°$.

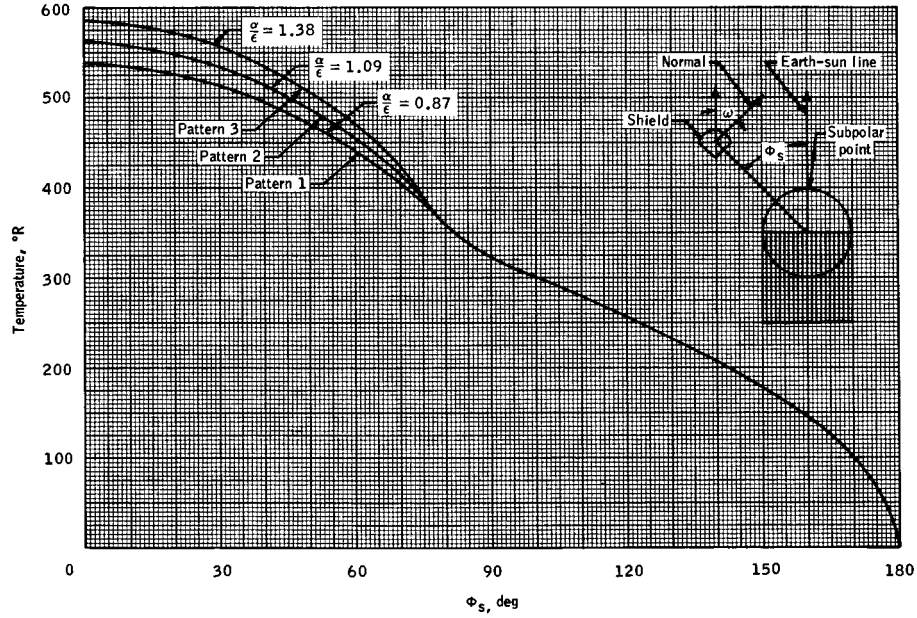

(e) $\omega = 150°$.

Figure 7. - Concluded.

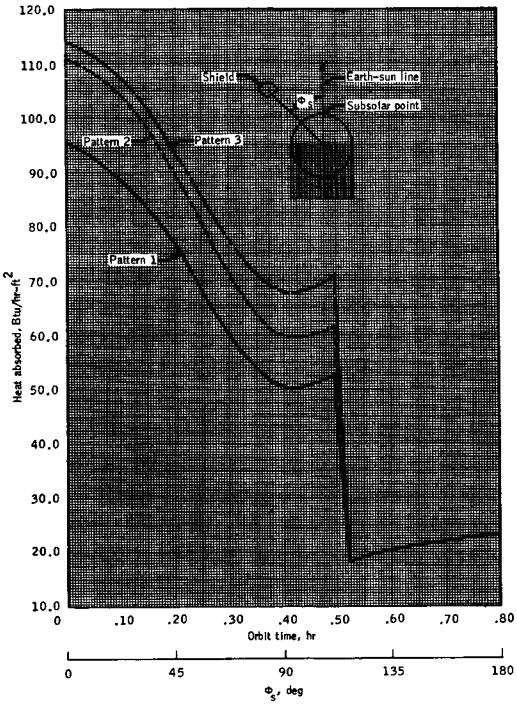

Figure 8. - Average external heat absorbed by shield of radial configuration. (See table III for pattern data.)

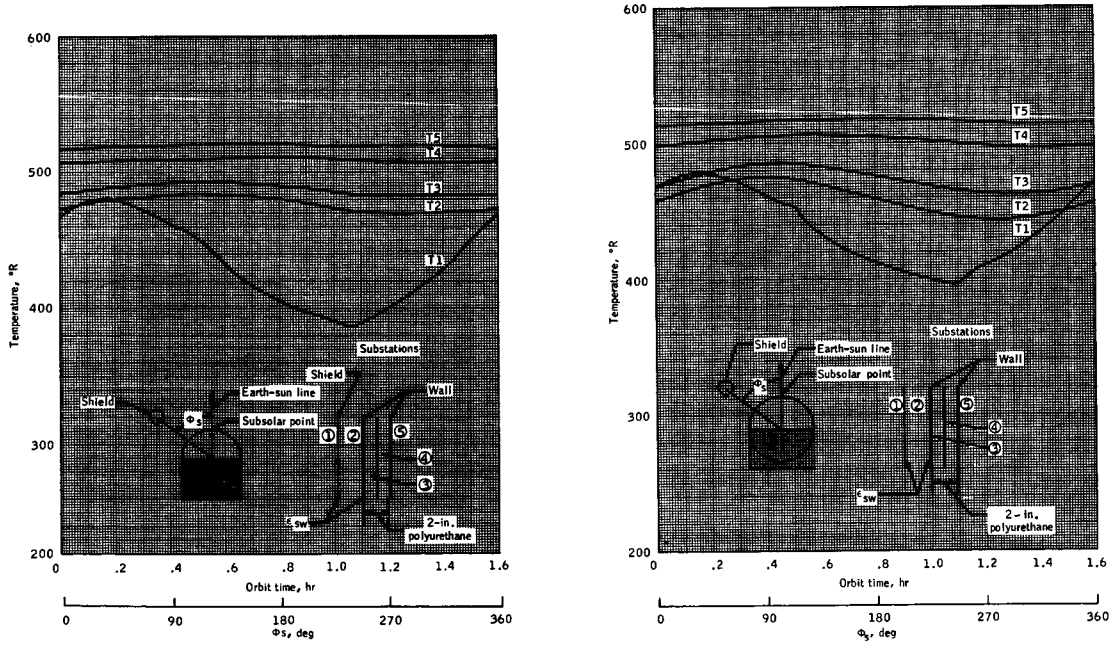

(a) $\epsilon_{SW} = 0.30$. (b) $\epsilon_{SW} = 0.90$.

Figure 9. - Radial configuration transient temperature profile for coating pattern 1.

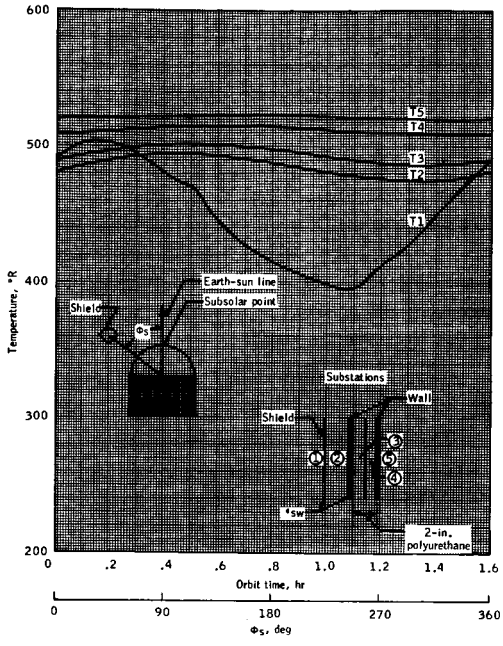

(a) $\epsilon_{SW} = 0.30$.

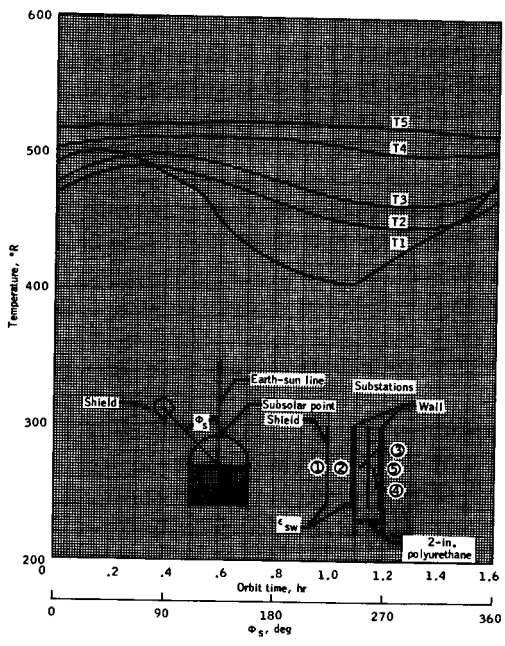

(b) $\epsilon_{SW} = 0.90$.

Figure 10. - Radial configuration transient temperature profile for coating pattern 2.

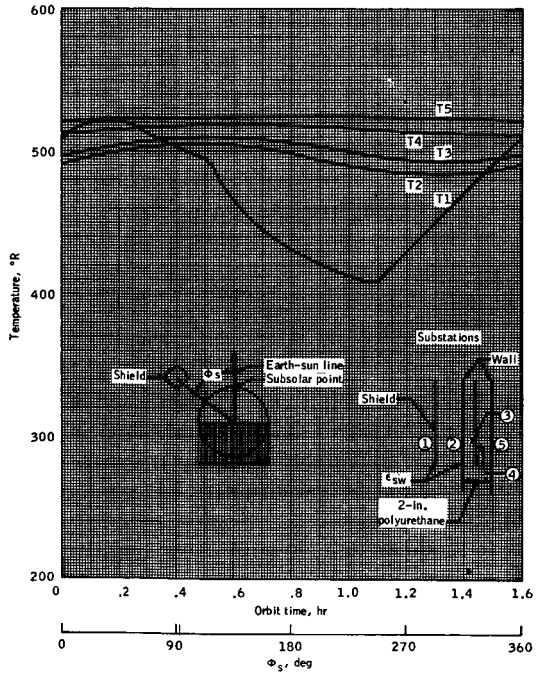

(a) $\epsilon_{SW} = 0.30$.

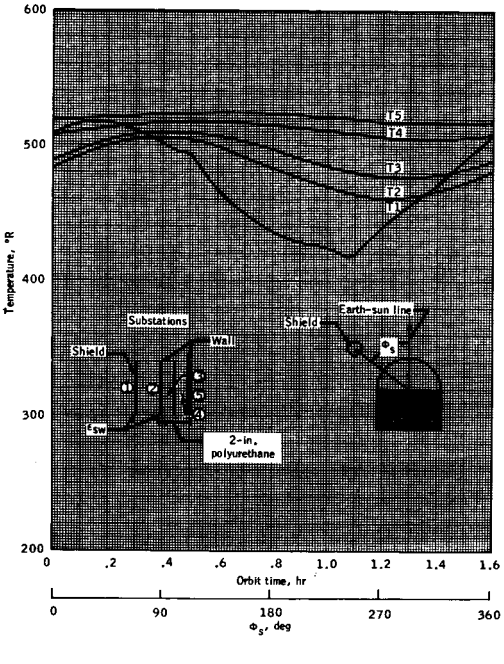

(b) $\epsilon_{SW} = 0.90$.

Figure 11. - Radial configuration transient temperature profile for coating pattern 3.

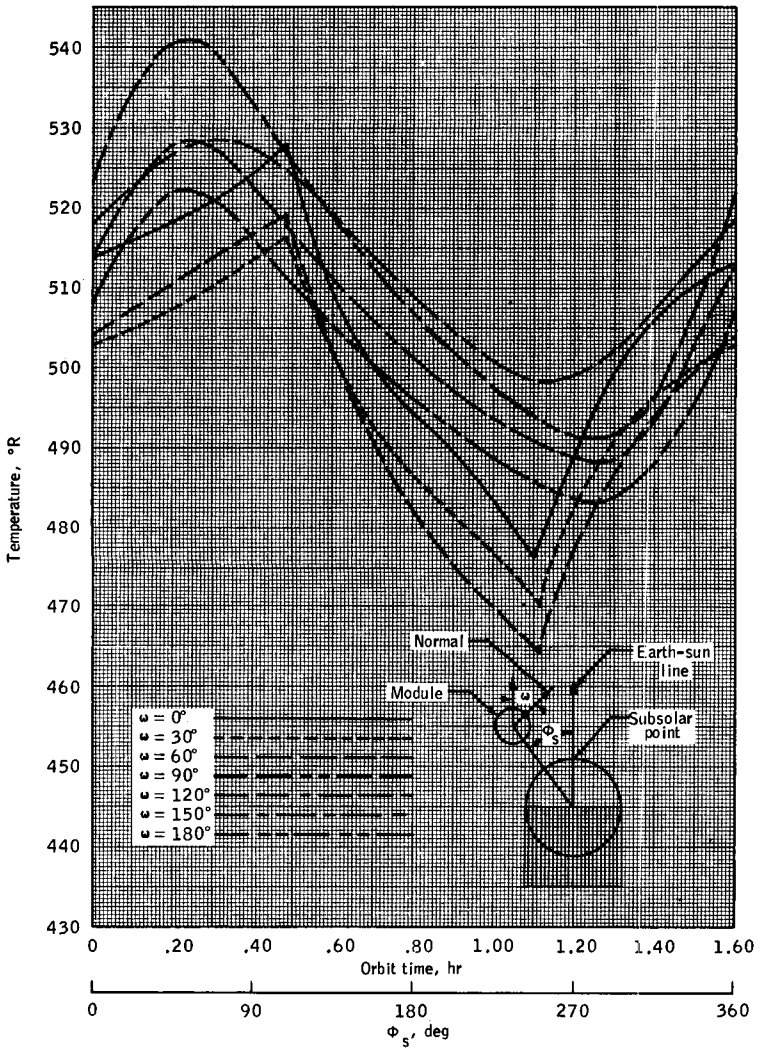

Figure 12. - LRC configuration transient temperature profile for power levels 1 and 2. (See table VI for surface characteristics.)

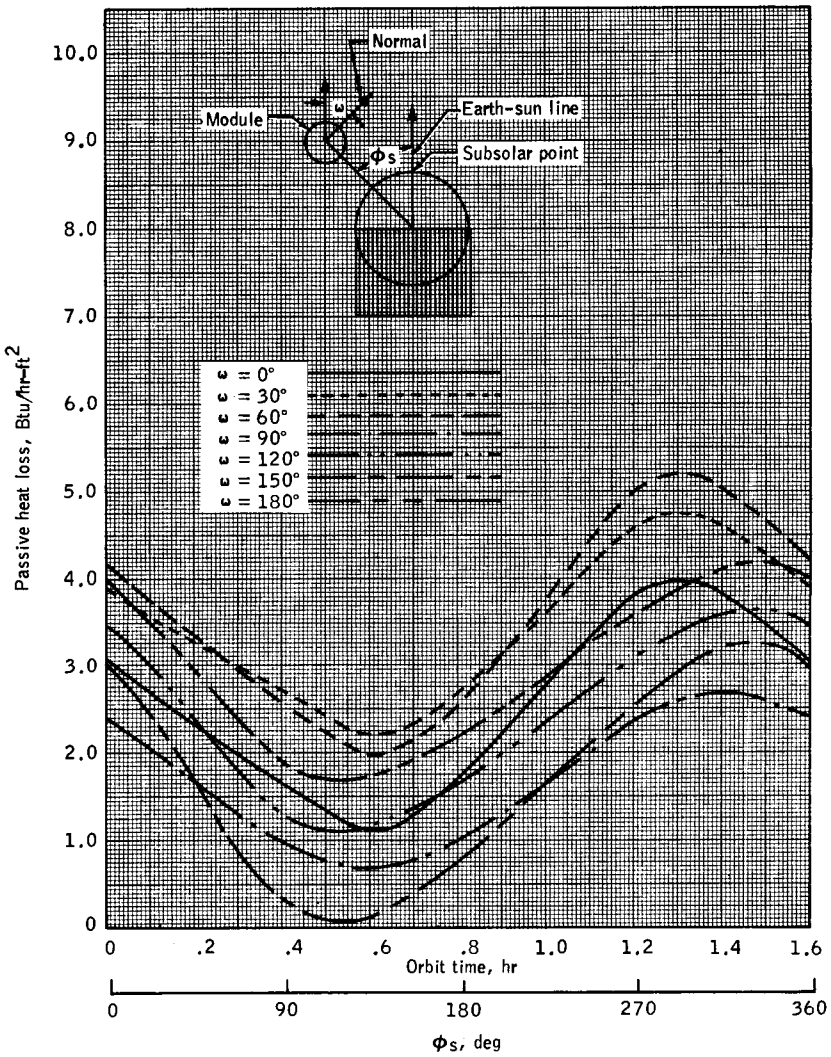

Figure 13. - LRC configuration passive heat loss profile for power levels 1 and 2. (See table VI for surface characteristics.)

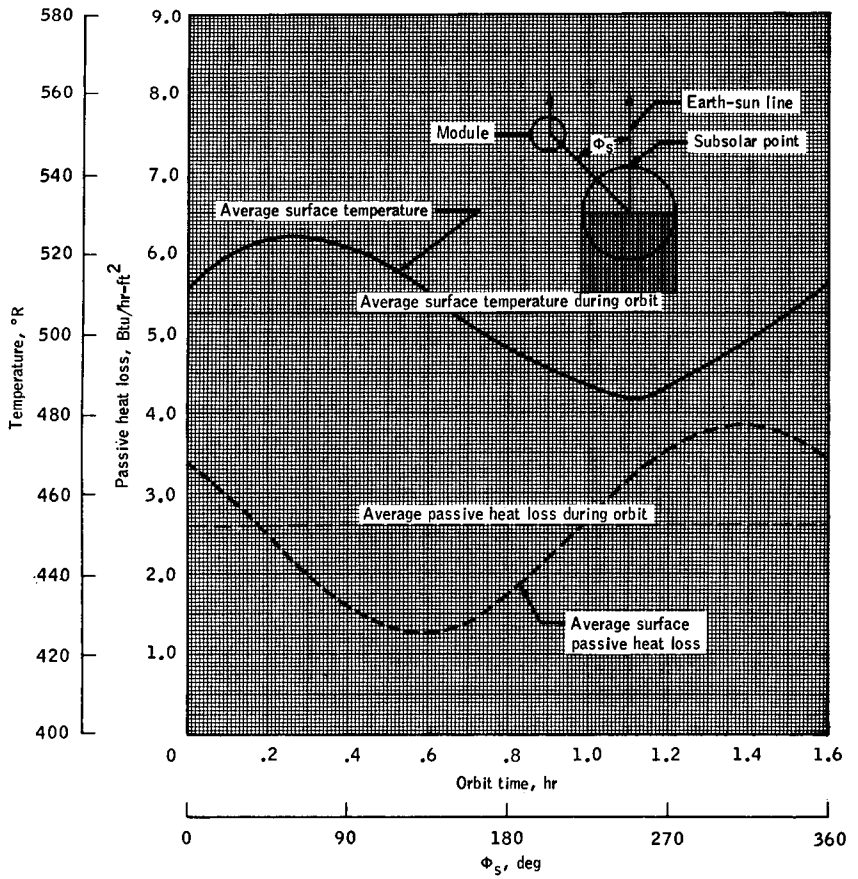

Figure 14. - LRC configuration average transient temperature and average passive heat loss for power levels 1 and 2. (See table VI for surface characteristics.)

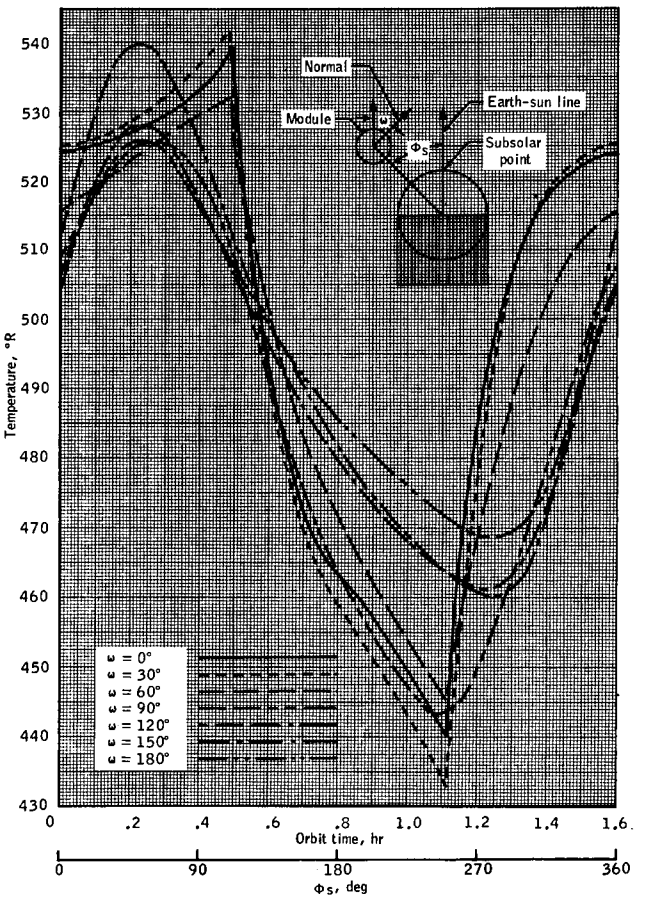

Figure 15. - LRC configuration transient temperature profile for power level 3. (See table VI for surface characteristics.)

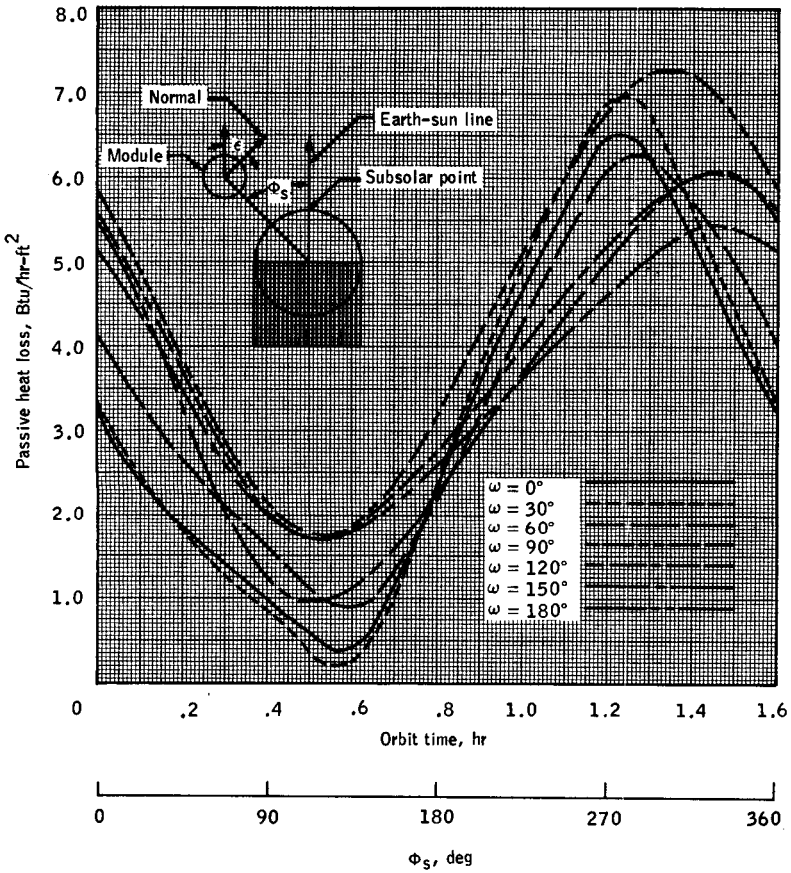

Figure 16. - LRC configuration passive heat loss profile for power level 3. (See table IV for surface characteristics.)

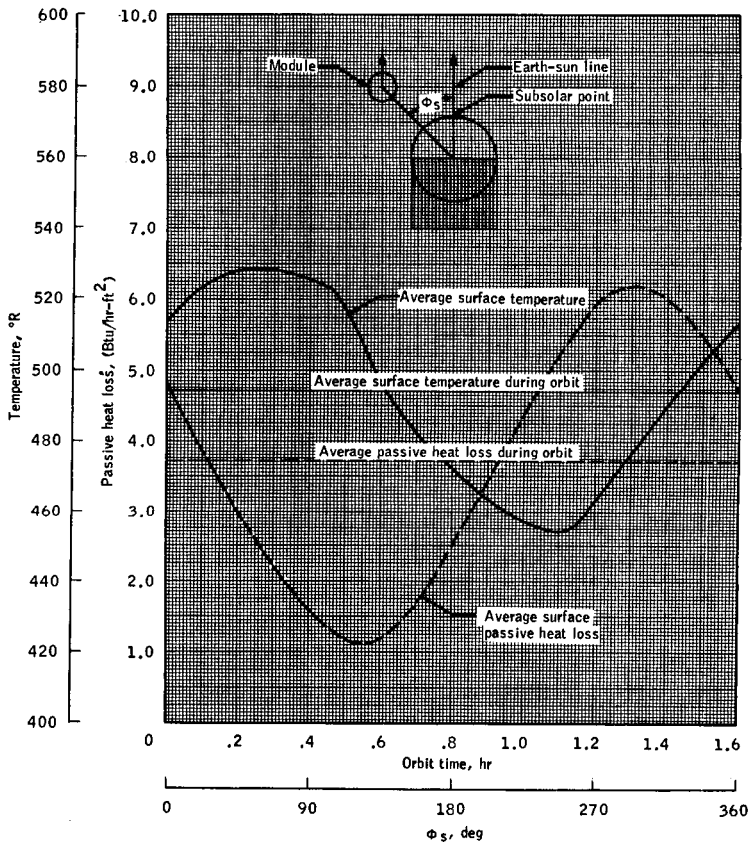

Figure 17. - LRC configuration average transient temperature and average passive heat loss for power level 3. (See table VI for surface characteristics.)

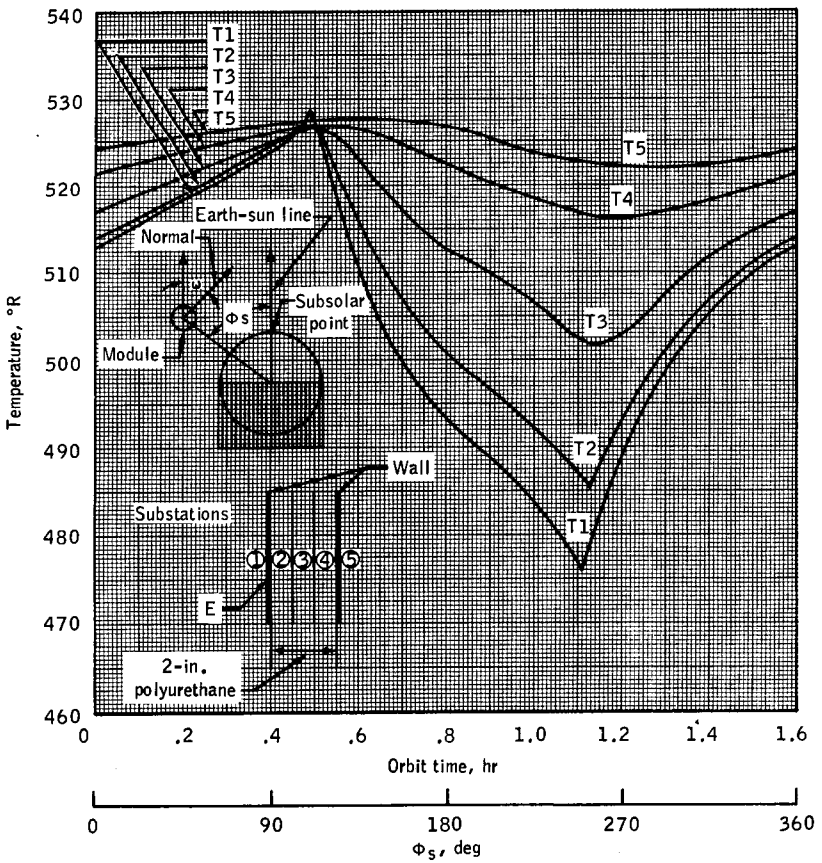

(a) $\omega = 0°$, $\frac{\alpha}{\epsilon} = 0.30$, $\epsilon = 0.30$.

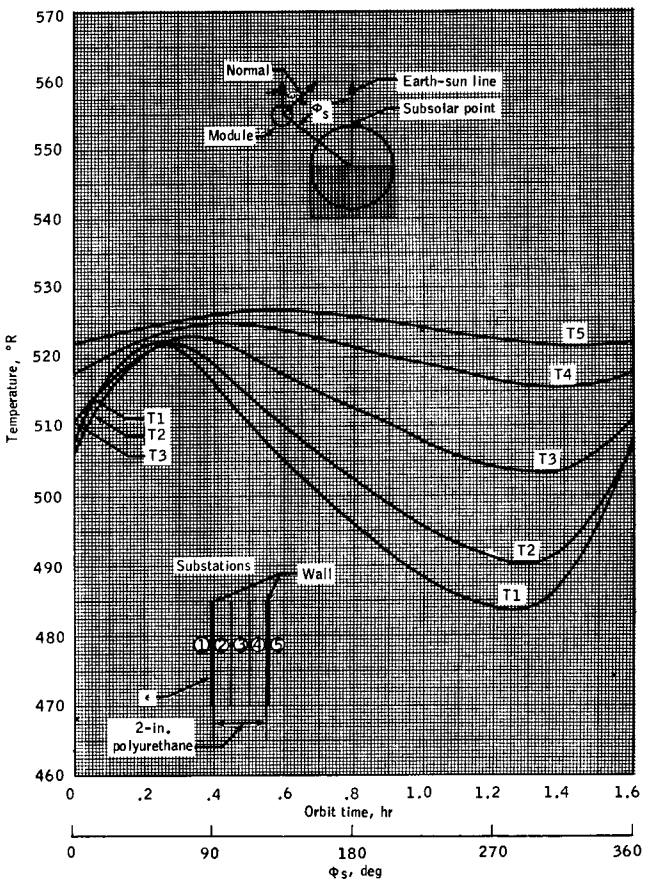

(b) $\omega = 180°$, $\frac{\alpha}{\epsilon} = 1.50$, $\epsilon = 0.10$.

Figure 18. - Typical transient wall temperature for LRC configuration.

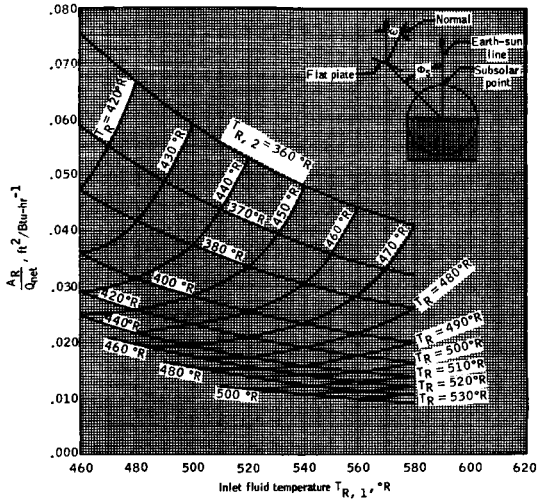

(a) $\omega = 90°$, $\frac{\alpha}{\epsilon} = 0.20$, $\epsilon = 0.90$, environmental sink temperature = 350° R.

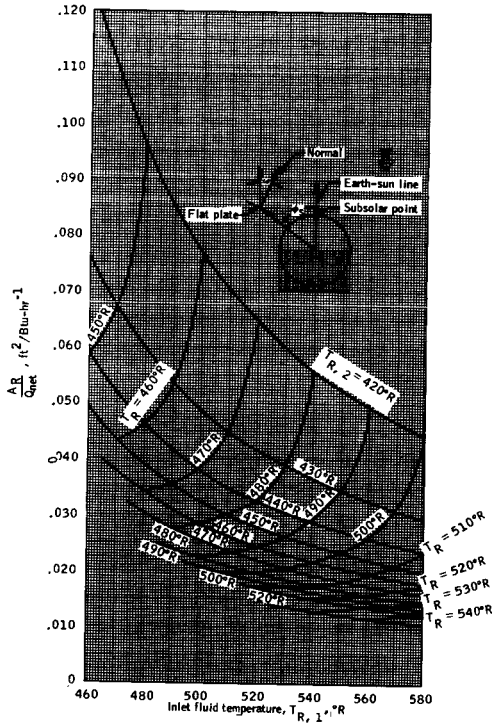

(b) $\omega = 150°$, $\frac{\alpha}{\epsilon} = 0.20$, $\epsilon = 0.90$, environmental sink temperature = 415° R.

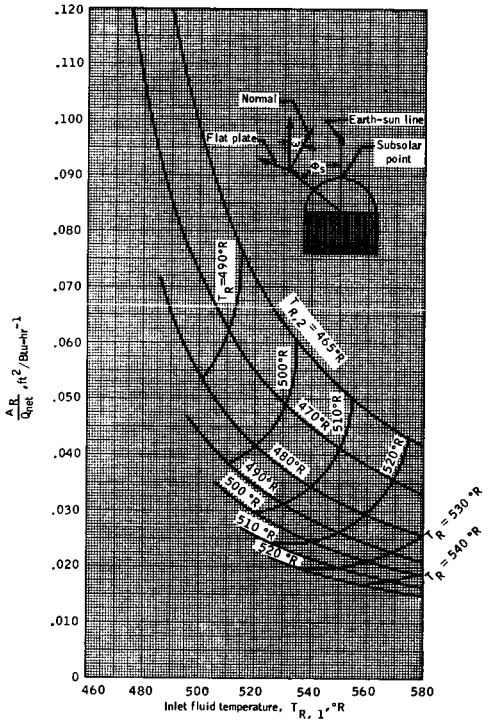

(c) $\omega = 180°$, $\frac{\alpha}{\epsilon} = 0.20$, $\epsilon = 0.90$, environmental sink temperature = 460° R.

Figure 19. - Flat plate radiator area per unit of heat rejection $\left(\frac{A_R}{Q_{net}}\right)$.

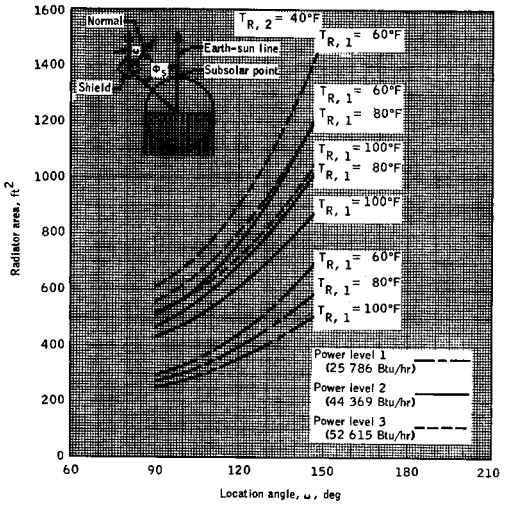

(a) Radial configuration.

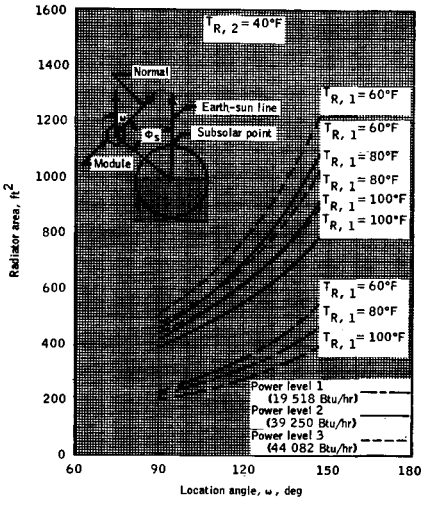

(b) LRC configuration.

Figure 20. - Radiator areas for maximum heat loads.

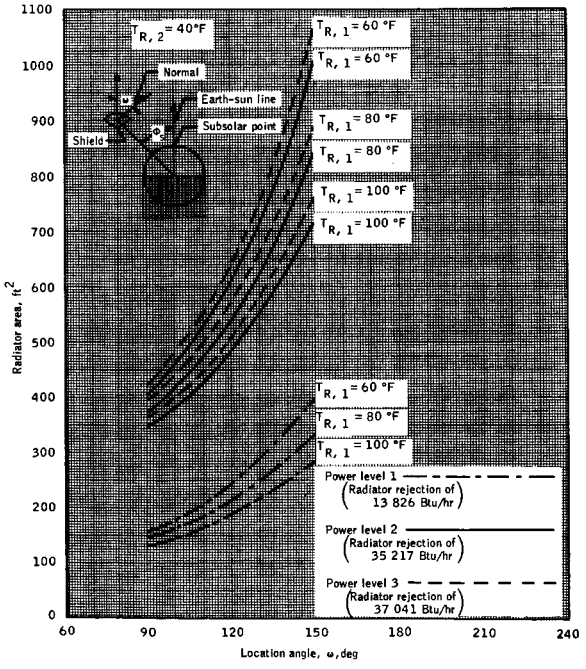

(a) Radial configuration.

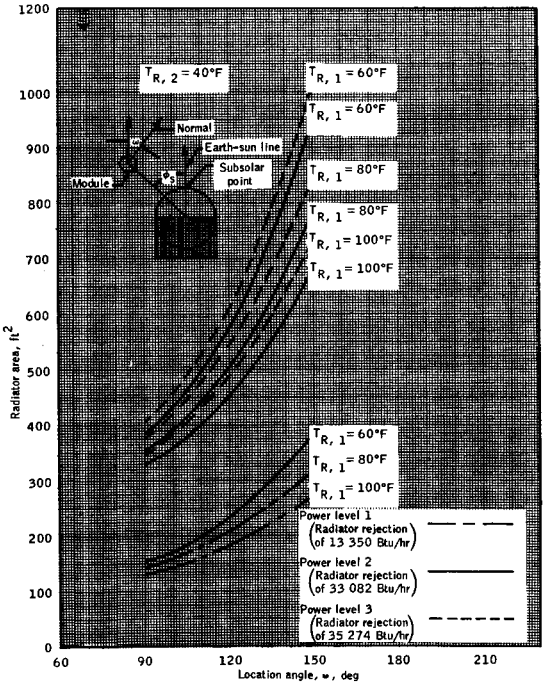

(b) LRC configuration.

Figure 21. - Radiator areas with passive heat loss from module.

NASA-Langley, 1967 —— 5 S-112